Adaptive Observation Strategy for Dispersion Process Estimation Using Cooperating Mobile Sensors[*]

Tobias Ritter [*,**] **Juliane Euler** [**] **Stefan Ulbrich** [*,***]
Oskar von Stryk [*,**]

[*] *Graduate School CE, TU Darmstadt, Germany*
[**] *Department of Computer Science, TU Darmstadt, Germany*
[***] *Department of Mathematics, TU Darmstadt, Germany*
(e-mail: ritter@gsc.tu-darmstadt.de,
{euler,stryk}@sim.tu-darmstadt.de,
ulbrich@mathematik.tu-darmstadt.de)

Abstract: Efficient online state estimation of dynamic dispersion processes plays an important role in a variety of safety-critical applications. The use of mobile sensor platforms is increasingly considered in this context, but implies the generation of situation-dependent vehicle trajectories providing high information gain in real-time.
In this paper, a new adaptive observation strategy is presented combining state estimation based on partial differential equation models of the dispersion process with a model-predictive control approach for multiple cooperating mobile sensors. In a repeating sequential procedure, based on the Ensemble Transform Kalman Filter, the uncertainty of the current estimate is determined and used to find valuable measurement locations. Those serve as target points for the controller providing optimal trajectories subject to the vehicles' motion dynamics and cooperation constraints. First promising results regarding accuracy and efficiency were obtained.

Keywords: Environmental monitoring, Adaptive observation, State estimation, PDE model, Mobile sensors, Cooperative control

1. INTRODUCTION

Whenever hazardous material spreads in the atmosphere, health and well-being of nature and humankind is at risk. For disaster response, it is essential to repeatedly estimate the state of the dispersion process to be able to understand its characteristics and to predict possible future impacts. For state estimation, a significant amount of information is required and the use of robotic systems for autonomous data gathering is increasingly considered in environmental monitoring (Dunbabin and Marques, 2012). Sensor-equipped autonomous vehicles are able to adapt their movement to a changing environment, which is particularly beneficial when dealing with large-scale, highly dynamic processes like atmospheric dispersion. However, a single mobile sensor is not able to cope with these process characteristics. Multiple sensor vehicles can cover larger domains and cooperate efficiently when controlled in an optimal manner.

The dimensions of the endangered domain prohibit pattern-based sampling or global exploration. Rather, immediate processing of the gathered data and subsequent optimized selection of complementary measurement locations is required. This is also known as *Adaptive Observation*.

Information obtained from the sensors and the predictions of an underlying process model can be combined by a data assimilation method to estimate the current process state. In this way, uncertainties in the estimate stemming from observation noise and model errors can be reduced. Using a partial differential equation (PDE) model, more accurate forecasts can be obtained since the physics and the dynamic behavior of the dispersion process are considered.

In literature, many approaches exist that avoid detailed PDE models and instead use simple models, such as Gaussian processes (Stranders et al., 2009), qualitative models (Duckham et al., 2005) or simply no model at all (Simic and Sastry, 2003). These models can provide results in a very short time and are frequently used in distributed systems. However, as important characteristics of the process dynamics are not considered, only inaccurate approximations of the real process are possible.
Adaptive observation strategies based on PDE models are commonly used in large-scale systems, e.g. for numerical weather prediction. In this field, a number of different approaches, like the singular vector technique (Buizza and Montani, 1999), the gradient method (Daescu and Navon, 2003), the ensemble spread technique (Lorenz and Emanuel, 1998), or the Ensemble Transform Kalman Filter (Bishop, 2001), have been applied. Due to the huge system dimensions, though, vehicle dynamics are not considered

in these applications.

Only a few publications focus on adaptive observation strategies combining both PDE models and vehicle dynamics. While Ucinski (2004) and Song et al. (2007) work on parameter estimation, Zhang et al. (2011) and Hover (2009) consider state estimation problems in conjunction with data assimilation. All these approaches involve solving a sophisticated optimal control problem subject to the process model, the covariance evolution, and the vehicle dynamics. Solving such complex problems is hard and time-consuming, especially regarding the real-time requirements of the application. Demetriou and Ucinski (2011) try to circumvent the optimal control problem and propose a Lyapunov-based sensor guidance scheme that can be applied in real-time. The resulting sensor motion allows for collision avoidance and connectivity constraints, but cannot be considered optimal with respect to vehicle cooperation.

In this paper, a new adaptive observation strategy is proposed that combines the accuracy of PDE-based process models with the potential of a team of optimally cooperating mobile sensors for online state estimation of a dispersion process. State estimation and vehicle control are considered separate problems that are linked in a repeating sequential procedure. This results in a significant gain of computational efficiency compared to solving a complex optimal control problem incorporating both aspects.

The proposed approach applies the Ensemble Transform Kalman Filter for state and uncertainty estimation, whereas a Mixed Logical Dynamical based model-predictive controller is used to guide the sensor vehicles to their destinations. While both concepts are well-established in literature, the novelty of this contribution lies in their combination and in the interaction between them: Based on the state estimate's error covariance matrix, locations with maximum uncertainty are chosen as future measurement points. Those points are handed to the cooperative controller which ensures that the sensor vehicles approach these targets in an optimal manner. After assimilating the gathered data with the predicted model state, new measurement locations are determined depending on the uncertainty in the updated state estimate. Repeating this procedure iteratively improves the quality of the state estimate. The required measurements are obtained at optimal exploitation of the vehicles' cooperation and their physical capabilities.

The rest of the paper is organized as follows. In Section 2, the process model is introduced together with the Ensemble Transform Kalman Filter, before the cooperative vehicle controller is presented in Section 3. The proposed adaptive observation strategy combining the two aforementioned concepts is described in Section 4. After examining the strategy with a simple test case in Section 5, the paper is concluded in Section 6 by giving an outlook on future work.

2. MODEL AND STATE ESTIMATION

2.1 Process Model

The approach presented in this work is aimed to estimate the state of a dynamic transport process that can be described by a PDE of the form

$$\frac{\partial \chi}{\partial t} = f(\chi(t), \nabla \chi(t), \Delta \chi(t), \mathbf{w}(t), \nabla \mathbf{w}(t)), \qquad (1)$$

where χ represents the dispersing entity to be estimated and $\mathbf{w}$ the underlying velocity field. With the aid of a spatial discretization scheme like the finite difference or the finite element method, the solution of the PDE can be represented by the state vector $\boldsymbol{\chi}$, which contains values of χ at certain, discrete spatial positions. Applying a suitable time integration scheme, the state vector at time t_{i+1} can then be calculated from a model forecast of the state vector at time t_i according to

$$\boldsymbol{\chi}_{i+1}^{\boldsymbol{f}} = M_i[\boldsymbol{\chi}_i^{\boldsymbol{f}}]. \qquad (2)$$

The superscript $(\cdot)^{\boldsymbol{f}}$ implies the forecasted state and M_i is known as the model operator. In general, this solution is not equal to the true solution of the system. The true solution, denoted by the superscript $(\cdot)^{\boldsymbol{t}}$, is defined as

$$\boldsymbol{\chi}_{i+1}^{\boldsymbol{t}} = M_i[\boldsymbol{\chi}_i^{\boldsymbol{t}}] + \boldsymbol{\eta}_i, \qquad (3)$$

where $\boldsymbol{\eta}_i$ represents the model error, which is assumed to be Gaussian with known covariance $\mathbf{Q}_i$.

2.2 Observations and Data Assimilation

To alleviate uncertainty stemming from the model, the process is also measured by a network of sensors. At certain times t_j, all sensors take a measurement and the observation vector $\boldsymbol{\psi}_j^{\boldsymbol{o}}$ is described by the relation

$$\boldsymbol{\psi}_j^{\boldsymbol{o}} = H_j[\boldsymbol{\chi}_j^{\boldsymbol{t}}] + \boldsymbol{\epsilon}_j, \qquad (4)$$

where $\boldsymbol{\epsilon}_j$ represents the observation error, which is, similar to the model error, assumed to be Gaussian with known covariance $\mathbf{R}_j$. The observation operator H_j maps vectors from the state space onto the observation space and depends on the positions the sensors take their measurements at. Thus, H_j has to be updated in every step to account for the current sensor positions.

To combine results obtained from simulation and from observations, a data assimilation method has to be chosen. A very popular approach is the *Kalman Filter* (KF) (Kalman, 1960). It is a sequential method for linear systems calculating the mean state and the error covariance matrix $\mathbf{P}_j$ of the estimate. Basically, the KF consists of two steps. In the prediction step, state and error covariance are forecasted from one observation time to the next:

$$\boldsymbol{\chi}_j^{\boldsymbol{f}} = M_{j-1}[\boldsymbol{\chi}_{j-1}^{\boldsymbol{a}}] \qquad (5)$$

$$\mathbf{P}_j^{\boldsymbol{f}} = \mathbf{M}_{j-1}\mathbf{P}_{j-1}^{\boldsymbol{a}}\mathbf{M}_{j-1}^T + \mathbf{Q}_{j-1}. \qquad (6)$$

When new observations are available, the update step has to be executed yielding the analysis (superscript $(\cdot)^{\boldsymbol{a}}$) mean state and error covariance matrix:

$$\boldsymbol{\chi}_j^{\boldsymbol{a}} = \boldsymbol{\chi}_j^{\boldsymbol{f}} + \mathbf{K}_j(\boldsymbol{\psi}_j^{\boldsymbol{o}} - H_j[\boldsymbol{\chi}_j^{\boldsymbol{f}}]) \qquad (7)$$

$$\mathbf{P}_j^{\boldsymbol{a}} = (\mathbf{I} - \mathbf{K}_j\mathbf{H}_j)\mathbf{P}_j^{\boldsymbol{f}}. \qquad (8)$$

While the matrices $\mathbf{M}_j$ and $\mathbf{H}_j$ are the linear model and observation operator, the matrix $\mathbf{K}_j$ is known as the Kalman gain and has to be calculated in every step according to

$$\mathbf{K}_j = \mathbf{P}_j^{\boldsymbol{f}}\mathbf{H}_j^T \left(\mathbf{H}_j\mathbf{P}_j^{\boldsymbol{f}}\mathbf{H}_j^T + \mathbf{R}_j\right)^{-1}. \qquad (9)$$

This choice of the Kalman gain minimizes the analysis error covariance matrix. However, the computation of $\mathbf{K}_j$

and especially the propagation of the error covariance matrix requires a huge amount of matrix multiplications and inversions. Thus, the KF is computationally not tractable for high dimensional systems, which are common in the considered application areas.

A modification of the KF called *Ensemble Kalman Filter* (EnKF) (Evensen, 1994) can avoid this problem. Here, a set of state vectors $(\boldsymbol{\chi}_j^1, \boldsymbol{\chi}_j^2, ..., \boldsymbol{\chi}_j^N)$ is considered. Starting from a perturbation of the initial guess, each single state vector is forecasted and updated, respectively, using perturbed observations. The main benefit of this method relies on the fact that the error covariance matrix does not have to be propagated explicitly. Instead, the deviation of the single ensemble members from the ensemble mean

$$\mathbf{Z}_j^{\boldsymbol{f}} = \frac{[\boldsymbol{\chi}_j^{\boldsymbol{f},1} - \overline{\boldsymbol{\chi}}_j^{\boldsymbol{f}}, \boldsymbol{\chi}_j^{\boldsymbol{f},2} - \overline{\boldsymbol{\chi}}_j^{\boldsymbol{f}}, \ldots, \boldsymbol{\chi}_j^{\boldsymbol{f},N} - \overline{\boldsymbol{\chi}}_j^{\boldsymbol{f}}]}{\sqrt{N-1}} \quad (10)$$

with

$$\overline{\boldsymbol{\chi}}_j^{\boldsymbol{f}} = \frac{\sum_k \boldsymbol{\chi}_j^{\boldsymbol{f},k}}{N} \quad (11)$$

is used to approximate the error covariance matrix

$$\mathbf{P}_j^{\boldsymbol{f}} = \mathbf{Z}_j^{\boldsymbol{f}} \mathbf{Z}_j^{\boldsymbol{f}T}. \quad (12)$$

Note that in (10)-(12) the superscript $(\cdot)^{\boldsymbol{f}}$ can be replaced by $(\cdot)^{\boldsymbol{a}}$ to calculate the analysis error covariance matrix accordingly. Typically, the ensemble size is much smaller than the state dimension and so this method is much more efficient than the KF. However, the data assimilation method to be used in this work should be capable to compute the analysis error covariance matrix before the actual measurements are taken. This is not the case for the EnKF since the provided analysis error covariance matrix depends on the observation vector.

Thus, a modification of the EnKF has to be made resulting in the *Ensemble Transform Kalman Filter* (ETKF) (Bishop, 2001). The idea of the ETKF approach is to express the analysis ensemble spread by the forecasted ensemble spread in the following way:

$$\mathbf{Z}_j^{\boldsymbol{a}} = \mathbf{Z}_j^{\boldsymbol{f}} \mathbf{T}_j. \quad (13)$$

Hence, unlike the EnKF approach, all ensemble members are updated together and deterministically. If it is assumed that (12) holds for the forecast error covariance matrix and (8) for the analysis error covariance matrix, the transformation matrix $\mathbf{T}$ fulfills

$$\mathbf{T}_j = \mathbf{V}_j(\boldsymbol{\Gamma}_j + \mathbf{I})^{-1/2}, \quad (14)$$

where $\mathbf{V}_j$ is the matrix of eigenvectors and $\boldsymbol{\Gamma}_j$ the corresponding matrix of eigenvalues of $\mathbf{Z}_j^{\boldsymbol{f}T} \mathbf{H}_j^T \mathbf{R}_j^{-1} \mathbf{H}_j \mathbf{Z}_j^{\boldsymbol{f}}$. From this, it is obvious that the ETKF enables the calculation of the analysis error covariance matrix before the actual measurements are available.

In most applications, the number of ensemble members is significantly lower than the dimension of the state enabling efficient computation of high dimensional problems. On the other hand, this discrepancy can lead to approximation problems like spurious correlations between distant locations and underestimation of the error covariance matrix. Localization (Houtekamer and Mitchell, 2001) and multiplicative inflation (Wang and Bishop, 2003) can be used to counteract these phenomena.

3. COOPERATIVE VEHICLE CONTROL

The cooperative feedback control approach presented in this section is able to guide multiple vehicles to a number of specified target locations that may change dynamically over time. Based on a linear discrete-continuous optimization scheme, it simultaneously determines collision-free vehicle trajectories as well as optimal target allocation respecting the vehicles' physical characteristics. The proposed controller can be adapted to various multi-vehicle constellations and task scenarios. Within the scope of this paper, it is applied to a homogeneous team of sensor vehicles and the number of target points is assumed to equal the number of vehicles.

3.1 MLD-Based Model-Predictive Control

The basic idea of the employed cooperative control approach is to set up a discrete-time linear *Mixed Logical Dynamical* (MLD) formulation of the considered multi-vehicle system, combine it with a suitable objective function, and solve the resulting optimal control problem

$$\min_{U_N} \ |\mathbf{F}\boldsymbol{x}^N| + \sum_{k=0}^{N-1} |\mathbf{G}_1\boldsymbol{u}^k| + |\mathbf{G}_2\boldsymbol{\delta}^k| + |\mathbf{G}_3\boldsymbol{z}^k| + |\mathbf{G}_4\boldsymbol{x}^k| \ \text{(15a)}$$

$$\text{s.t.} \qquad \boldsymbol{x}^{k+1} = \mathbf{A}\boldsymbol{x}^k + \mathbf{B}_1\boldsymbol{u}^k + \mathbf{B}_2\boldsymbol{\delta}^k + \mathbf{B}_3\boldsymbol{z}^k \qquad \text{(15b)}$$

$$\boldsymbol{y}^k = \mathbf{C}\boldsymbol{x}^k + \mathbf{D}_1\boldsymbol{u}^k + \mathbf{D}_2\boldsymbol{\delta}^k + \mathbf{D}_3\boldsymbol{z}^k \qquad \text{(15c)}$$

$$\mathbf{E}_2\boldsymbol{\delta}^k + \mathbf{E}_3\boldsymbol{z}^k \leq \mathbf{E}_1\boldsymbol{u}^k + \mathbf{E}_4\boldsymbol{x}^k + \mathbf{E}_5 \ , \qquad \text{(15d)}$$

in a receding horizon fashion to compute optimal control inputs for each vehicle. In this problem formulation, $\boldsymbol{x} = [\boldsymbol{x}_c \ \boldsymbol{x}_b]^T, \boldsymbol{x}_c \in \mathbb{R}^{n_c}, \boldsymbol{x}_b \in \{0,1\}^{n_b}$, is the system state, $\boldsymbol{y} = [\boldsymbol{y}_c \ \boldsymbol{y}_b]^T, \boldsymbol{y}_c \in \mathbb{R}^{p_c}, \boldsymbol{y}_b \in \{0,1\}^{p_b}$, is the output vector, $\boldsymbol{u} = [\boldsymbol{u}_c \ \boldsymbol{u}_b]^T, \boldsymbol{u}_c \in \mathbb{R}^{m_c}, \boldsymbol{u}_b \in \{0,1\}^{m_b}$, is the control input, and $\boldsymbol{\delta} \in \{0,1\}^{r_b}$ and $\boldsymbol{z} \in \mathbb{R}^{r_c}$ represent auxiliary binary and continuous vectors, respectively. The prediction time step $k = 0, \ldots, N-1$ relates to the global equidistant time steps $t_i \in \mathbb{N}$ according to $\boldsymbol{x}^k = \boldsymbol{x}(t_{i+k})$. As solution of problem (15), the sequence $U_N := \{\boldsymbol{u}^k\}_{k=0}^{N-1}$ of control inputs is obtained. In virtue of a model-predictive control (MPC) scheme, the first element of U_N is applied to the real system, then its new state is measured for computing updated control inputs at the next time step t_{i+1}. In this manner, the prediction horizon N is shifted over time.

The MLD framework (15b)–(15d) was proposed by Bemporad and Morari (1999) for modeling and controlling constrained linear systems containing interacting physical laws and logical rules. In this paper, it is used to describe both the motion of multiple mobile sensors and the decision logic required to ensure optimal target allocation among them as well as their adherence to distance constraints. The objective function (15a) can reflect a prioritization of different problem aspects. Problem (15) is a mixed-integer linear *Constrained Finite Time Optimal Control* (CFTOC) problem. It can easily be transformed into a *Mixed Integer Linear Program* (MILP) at each time step of the MPC procedure. Therefore, a numerically robust, efficient computation of control inputs can be performed. The modeling details will be given in Section 3.2.

The described control scheme is applied in a centralized manner for the global system of vehicles and measurement locations. Hence, globally optimal cooperative behavior

within the scope of the system model and the chosen prediction horizon N is obtained. However, the efficiency of the centralized MPC approach strongly depends on the size of the system model, i.e. the number of vehicles.

3.2 Modeling the Multi-Vehicle System

Motion Dynamics Employing the MLD framework (15b)–(15d) for modeling multi-vehicle systems permits to use all kinds of discrete-time linear motion dynamics models that can be stated in the form

$$\boldsymbol{x}_v^{k+1} = \mathbf{A}_v \boldsymbol{x}_v^k + \boldsymbol{B}_v \boldsymbol{u}_v^k , \qquad (16)$$

where $\boldsymbol{x}_v^k$ and $\boldsymbol{u}_v^k$ denote the state and control input, respectively, of vehicle $v \in \{1, \dots, n_V\}$ at time step k. Let $\boldsymbol{x}_V^k = (\boldsymbol{x}_1^k, \dots, \boldsymbol{x}_{n_V}^k)$ and $\boldsymbol{u}_V^k = (\boldsymbol{u}_1^k, \dots, \boldsymbol{u}_{n_V}^k)$.

It is assumed that measurement locations shift with the wind in order to best preserve their information level until reached by a sensor. Therefore, their movement is predicted according to a linearized representation of the advection influence

$$\boldsymbol{x}_m^{k+1} = \mathbf{A}_m \boldsymbol{x}_m^k + \boldsymbol{b}_m , \qquad (17)$$

where $\boldsymbol{x}_m^k$, $m \in \{1, \dots, n_M\}$, is the position of target m at time k. Let $\boldsymbol{x}_M^k = (\boldsymbol{x}_1^k, \dots, \boldsymbol{x}_{n_M}^k)$.

Distances A linear approximation d_{vm}^k of the Euclidean distance between a vehicle v and a measurement point m is obtained by introducing a set of inequalities

$$(x_v^k - x_m^k) \sin \frac{2\pi\gamma}{n_\gamma} + (y_v^k - y_m^k) \cos \frac{2\pi\gamma}{n_\gamma} \leq d_{vm}^k , \quad (18)$$

where (x_v^k, y_v^k) denotes the vehicle's position, (x_m^k, y_m^k) the measurement location at time k, and $\gamma = 1, \dots, n_\gamma$. If d_{vm}^k takes the minimum value such that all inequalities (18) hold, then $d_{vm}^k \approx \sqrt{(x_v^k - x_m^k)^2 + (y_v^k - y_m^k)^2}$. The accuracy of the approximation can be scaled by the constant parameter $n_\gamma \in \mathbb{N}$. Including a distance criterion in the objective function (15a) ensures that d_{vm}^k is driven to its smallest possible value whenever that value is relevant for the optimal solution.

Measurement Constraints For each pair (v, m), a binary variable $b_{vm}^k \in \{0, 1\}$ indicates whether or not vehicle v measures at target m at time k:

$$b_{vm}^k = 1 \quad \Leftrightarrow \quad d_{vm}^k \leq d_{meas} , \qquad (19)$$

where d_{meas} determines how close to $\boldsymbol{x}_m^k$ a vehicle has to be in order to trigger a measurement. A linear representation of (19) is given by the inequalities

$$d_{vm}^k - r_m \leq M_1(1 - b_{vm}^k) \quad \text{and} \qquad (20a)$$
$$d_{vm}^k - r_m \geq \varepsilon + (m_1 - \varepsilon) b_{vm}^k , \qquad (20b)$$

where $M_1 \geq \max\{d_{vm} - r_m\}$, $m_1 \leq \min\{d_{vm} - r_m\} = -r_m$, and ε is a small tolerance close to machine precision.

Since it is not of interest which sensor measures at target m, but that the measurement is eventually taken by any sensor, another binary variable $s_m^k \in \{0, 1\}$ is introduced and represents the measurement status of m:

$$s_m^k = 0 \quad \Leftrightarrow \quad \sum_{v=1}^{n_V} b_{vm}^k \geq 1 . \qquad (21)$$

Eq. (21) can be linearized by introducing the inequalities

$$1 - \sum_{v=1}^{n_V} b_{vm}^k \leq M_2 \cdot s_m^k \quad \text{and} \qquad (22a)$$

$$1 - \sum_{v=1}^{n_V} b_{vm}^k \geq \varepsilon + (m_2 - \varepsilon)(1 - s_m^k) , \qquad (22b)$$

where $M_2 \geq \max\{1 - \sum b_{vm}\} = 1$ and $m_2 \leq \min\{1 - \sum b_{vm}\} = 1 - n_V$.

Cooperation among the sensor vehicles is realized by minimizing the number of unprocessed measurement locations, i.e. $\sum_{m=1}^{n_M} s_m^k$, and each vehicle's distance to those locations not yet visited by any other vehicle. The latter is expressed using the variables s_m and an additional set of auxiliary variables $h_{vm} \in \mathbb{R}$ that either equal the distances d_{vm} or zero, depending on the status of target m:

$$h_{vm}^k = s_m^k \cdot d_{vm}^k . \qquad (23)$$

The linear representation of (23) comprises the inequalities

$$h_{vm}^k \leq M_3 \cdot s_m^k , \qquad (24a)$$
$$h_{vm}^k \leq d_{vm}^k , \quad \text{and} \qquad (24b)$$
$$-h_{vm}^k \leq -d_{vm}^k + M_3(1 - s_m^k) , \qquad (24c)$$

where $M_3 \geq \max\{d_{vm}\}$.

Collision Avoidance In order to make every two vehicles v_i and v_j, $i \neq j$, keep a minimum distance d_{min} to each other, they should avoid the region defined by

$$(x_{v_i}^k - x_{v_j}^k) \sin_\gamma + (y_{v_i}^k - y_{v_j}^k) \cos_\gamma \leq d_{min} , \qquad (25)$$

where $\sin_\gamma := \sin \frac{2\pi\gamma}{n_\gamma}$ and $\cos_\gamma := \cos \frac{2\pi\gamma}{n_\gamma}$.

Hence, at least one of the inequalities (25) must be violated, which can be expressed by the following logical rules involving an additional set of binary variables $b_{ij\gamma}^k$:

$$(x_{v_i}^k - x_{v_j}^k) \sin_\gamma + (y_{v_i}^k - y_{v_j}^k) \cos_\gamma > d_{min} \Rightarrow b_{ij\gamma}^k = 0 \quad (26)$$

$$\text{and} \quad \sum_{\gamma=1}^{n_\gamma} b_{ij\gamma}^k \leq n_\gamma - 1 . \qquad (27)$$

Linearizing (26) yields

$$(x_{v_j}^k - x_{v_i}^k) \sin_\gamma + (y_{v_j}^k - y_{v_i}^k) \cos_\gamma \leq -d_{min} + M_4 \cdot b_{ij\gamma}^k , \quad (28)$$

where $M_4 \geq \max\{(x_{v_j}^k - x_{v_i}^k) \sin_\gamma + (y_{v_j}^k - y_{v_i}^k) \cos_\gamma + d_{min}\}$.

Objectives The controller's main purpose is to lead each vehicle to one of the measurement locations, which is represented in the objective function as minimization of the distances h_{vm}^k as well as the binary variables s_k^k. In addition, the vehicles are to move at a minimum control effort, which in reality could correspond to energy consumption or other limiting factors. In summary, the cost function takes the form:

$$\min_{U_N} \sum_{k=0}^{N-1} \Big(g_z \sum_{v=1}^{n_V} \sum_{m=1}^{n_M} h_{vm}^k + g_\delta \sum_{m=1}^{n_M} s_m^k + g_u |\boldsymbol{u}_V^k| \Big) , \qquad (29)$$

where g_z, g_δ, $g_u \in \mathbb{R}$ weight the different objectives according to their priorities and the best expected task performance.

The objective function (29) subject to (16)-(18), (20), (22), (24), and (27)-(28) can be reformulated as CFTOC problem (15) in order to apply the MPC approach as outlined in section 3.1. In this representation, the vector

$\boldsymbol{x}^k$ contains the state of all n_V vehicles as well as the n_M measurement locations. All binary variables are contained in $\boldsymbol{\delta}^k \in \{0, 1\}^{(n_V+1)n_M + \binom{n_V}{2}n_\gamma}$. $\boldsymbol{z}^k \in \mathbb{R}^{2n_V n_M}$ comprises the approximated distances d_{vm}^k and h_{vm}^k. The vector $\boldsymbol{u}^k$ summarizes the vehicle control inputs. The overall problem comprises $n_V n_M (5 + n_\gamma) + 4n_M + \binom{n_V}{2}(n_\gamma + 1)$ linear inequality constraints.

4. ADAPTIVE OBSERVATION STRATEGY

This section describes how the ETKF-based state and uncertainty estimation (cf. Section 2) is combined with the model-predictive vehicle controller (cf. Section 3) to obtain an efficient optimization-based adaptive observation strategy. A schematic overview over the proposed method is given in Figure 1, Algorithm 1 shows the procedure during one time step in more detail. While the ETKF can provide several measures of current uncertainty and of future measurements' impact on estimate quality, the controller requires discrete target points to guide the sensor vehicles to. Therefore, a method to generate these target points with the aid of the ETKF has been developed and is described in the following.

The error covariance matrix provided by the ETKF is a suitable measure of the quality of a state estimate. Large entries indicate high uncertainties and, thus, high deviations between true state and estimate. The objective is to iteratively improve the state estimate of the considered dispersion process, i.e. to reduce the entries in the covariance matrix. This can be achieved by taking measurements at positions where the uncertainty in the estimate is largest and the most valuable information can be obtained. As these positions are likely to change due to the dynamic process behavior and the incorporation of gathered data, the vehicles' target points have to be updated from time to time.

In order to determine the target points $\boldsymbol{x}_M$, the current error covariance matrix $\mathbf{P}^a$ is calculated applying the ETKF. To obtain the largest possible reduction of the covariance matrix, the measurement points should be chosen in dependence of the eigenvector corresponding to the largest eigenvalue of the covariance matrix. However, as it is not straightforward to generate the measurement locations out of the eigenvector, a simpler approach is used considering the diagonal of the matrix, i.e. the variance of the state vector entries. The location $\boldsymbol{x}_{\max}$ that belongs to the maximum value of the diagonal is chosen as the first measurement location $\boldsymbol{x}_M^1 = \boldsymbol{x}_1 = \boldsymbol{x}_{\max}$. Hence, the new target point is not determined by continuous optimization, but by finding the maximum from a discrete set of candidates. This is not necessarily the optimal position at which measurements are most valuable – however, this choice provides a fast and suitable approximation. Further target points are calculated iteratively in the same manner, but considering the analysis error covariance matrix $\tilde{\mathbf{P}}^a$. The latter is calculated by the ETKF pretending that observations are available at all previously calculated target points. Therefore, the observation matrix $\tilde{\mathbf{H}}^k$ has to be determined in every iteration k from the vector $\boldsymbol{x}_M^{k-1} = (\boldsymbol{x}_1, \ldots, \boldsymbol{x}_{k-1})$. By using the analysis error covariance, clusterization of target points in regions with high uncertainty is avoided.

As the covariance changes in time, it is obvious that the quality of the target points continuously reduces until reached by a sensor vehicle. Still, the targets will not be recalculated at every time step. Instead, they are moved according to the underlying wind velocity since it is assumed that the characteristic evolution of the covariance matrix is directed with the wind. This prevents the target points from jumping from one position to another and guarantees that they can actually be reached by the sensors.

As soon as one of the sensors reaches a measurement location, all sensors take a measurement, the state estimation is updated, and new target points are generated. It is likely that at that time, the other sensors have not reached their targets, yet. However, the benefit of a measurement close to the optimal location and an earlier update of all observation targets is greater than waiting for them to arrive at a possibly outdated destination.

In general, the sensor platforms in the proposed approach only take measurements if a sensor is located at a target position. At all intermediate times, no observation is made. Although additional measurements on the way would probably further improve the results, the larger measurement intervals are still sufficient to provide much better results than other strategies with more frequent measurements (see Section 5).

Algorithm 1 Adaptive observation time step at $t = t_i$

$[\boldsymbol{\chi}_i^f, \mathbf{P}_i^f] \leftarrow$ FORECAST PROCESS$(\boldsymbol{\chi}_{i-1}^a, \mathbf{P}_{i-1}^a)$
$\boldsymbol{x}_{V,i} \leftarrow$ UPDATE VEHICLE STATES$(\boldsymbol{x}_{V,i-1}, \boldsymbol{u}_{V,i-1}^0)$
if new observation $\boldsymbol{\psi}_i^o$ available **then**
$\quad \mathbf{H}_i \leftarrow$ OBSERVATION MATRIX$(\boldsymbol{x}_{V,i})$
$\quad [\boldsymbol{\chi}_i^a, \mathbf{P}_i^a] \leftarrow$ ETKF$(\boldsymbol{\chi}_i^f, \mathbf{P}_i^f, \boldsymbol{\psi}_i^o, \mathbf{H}_i)$
$\quad \boldsymbol{x}_{M,i}^0 \leftarrow ()$
$\quad$ **for** $k \leftarrow 1$ to n_V **do**
$\quad\quad \tilde{\mathbf{H}}_i^k \leftarrow$ OBSERVATION MATRIX$(\boldsymbol{x}_{M,i}^{k-1})$
$\quad\quad \tilde{\mathbf{P}}_i^{a,k} \leftarrow$ ETKF COVARIANCE$(\mathbf{P}_i^a, \tilde{\mathbf{H}}_i^k)$
$\quad\quad \boldsymbol{x}_{\max} \leftarrow$ location belonging to max$(\text{diag}(\tilde{\mathbf{P}}_i^{a,k}))$
$\quad\quad \boldsymbol{x}_{M,i}^k \leftarrow (\boldsymbol{x}_{M,i}^{k-1}, \boldsymbol{x}_{\max})$
$\quad$ **end for**
$\quad \boldsymbol{x}_{M,i} \leftarrow \boldsymbol{x}_{M,i}^{n_V}$
else
$\quad \boldsymbol{x}_{M,i} \leftarrow$ MOVE IN WIND DIRECTION$(\boldsymbol{x}_{M,i-1})$
end if
$\boldsymbol{u}_{V,i}^0 \leftarrow$ CONTROLLER$(\boldsymbol{x}_{V,i}, \boldsymbol{x}_{M,i})$

---

5. RESULTS

In order to illustrate the proposed approach, a simple test case is set up considering a 2D problem on a 4×2 domain. The dispersion process is assumed to be governed by the source-free linear advection-diffusion equation

$$\frac{\partial c}{\partial t} + \nabla \cdot (c\mathbf{w}) - \nabla \cdot (\mathbf{D}\nabla c) = 0, \tag{30}$$

where the function c, representing the concentration, is to be estimated. The diffusion matrix $\mathbf{D}$ is assumed to be homogeneous and constant and the velocity field $\mathbf{w}$ is uniform with $w_1 = 0.005$ in x-direction and a vanishing component in y-direction. The finite element method is used to solve (30). As the considered problems are highly advection dominated, the application of a
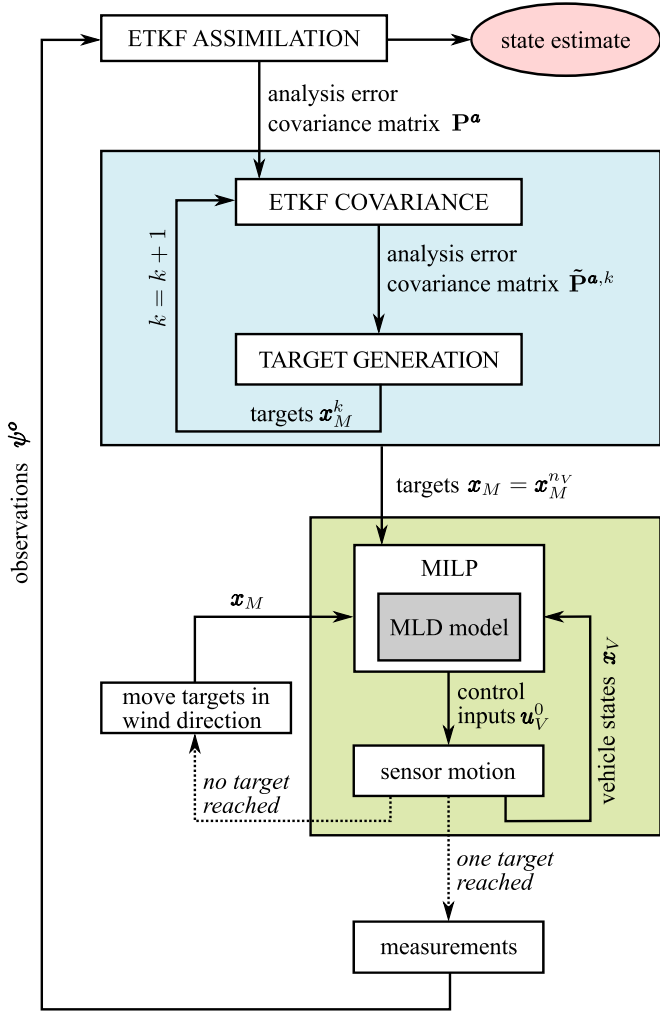
Fig. 1. Schematic view of the proposed adaptive observation strategy.

Fig. 2. Comparison of the mean estimation error over time for three different sensor movement strategies.

(a) True state   (b) Estimated state

Fig. 3. Concentration field at $t = 240$.

standard Galerkin method might lead to instabilities. Therefore, a characteristic Galerkin method is applied.

A so-called twin experiment is performed to provide the observations considered in this test case, i.e. the true solution is assumed to be known and is forecasted in time according to (3). From this, observations are obtained using (4). The difference between the true solution and the estimated solution resides in their initial condition. While the initial estimate has the form of a simple Gaussian pulse

$$c_0(x,y) = c_A \exp\left(-\left(\frac{(x-x_0)^2}{2\sigma_x^2} + \frac{(y-y_0)^2}{2\sigma_y^2}\right)\right) \quad (31)$$

with amplitude $c_A = 1$ centered at $(x_0,y_0) = $ (-1,0), the initial true state is assumed to be composed of three Gaussian pulses with perturbed parameters.

Three sensor vehicles modeled as point masses with a maximum velocity and acceleration of 0.02 are employed. Thus, the sensors are four times faster than the characteristic process speed, enabling them to reach every calculated target point. To avoid collisions and redundant measurements, the minimum distance between two sensors is set to 0.1. Their initial positions are (-0.2,-0.4), (0.2,-0.4), and (0,-0.2), respectively. An MPC prediction horizon of $N = 15$ time steps is used, while $\Delta t = 2$ is assumed.
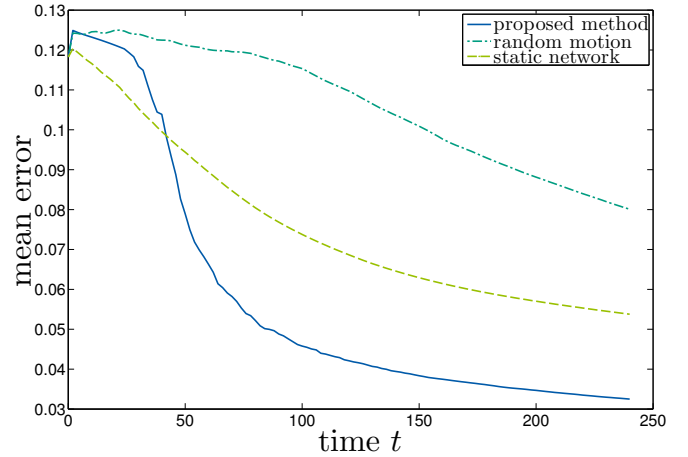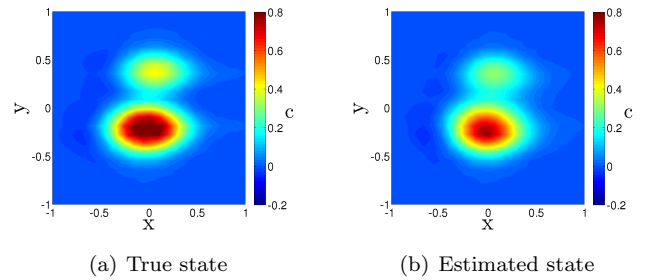
In order to compare the performance of the proposed approach, two other sensor configurations are applied in the same problem setup. The first consists of three mobile sensors that move randomly, whereas the second employs 16 static sensors evenly distributed in a square area from (-0.6,-0.6) to (0.6,0.6). In both configurations, each sensor takes a measurement every time step.

The test scenario was run 50 times for 120 time steps, each time with a different randomly chosen initial true state. As the true solution is assumed to be known, the quality of the resulting state estimates can be quantified considering their deviation from the true state. In this way, the error can be calculated at every time step by forming the norm of the deviation vector.

Figure 2 shows the evolution of the mean error over time for the three different observation strategies and Figure 3 depicts a comparison of the true and estimated state of the concentration field for an example test run after 120 time steps. Although the strategy proposed in this paper results in only ~ 75 measurements within the given time frame – five times less than for the random motion and even 26 times less than for the static sensors – it provides the least error. At $t = 240$, the estimation error obtained from the static sensor network is 1.5 times greater than the error obtained from the proposed adaptive observation strategy. The error obtained using random sensor motion is even 2.5 times greater.

Figure 4 depicts a snapshot of vehicle trajectories and measurement locations for an example test run. Typically, one sensor reaches a target point and invokes a measurement of all sensors. Although the other sensors are still
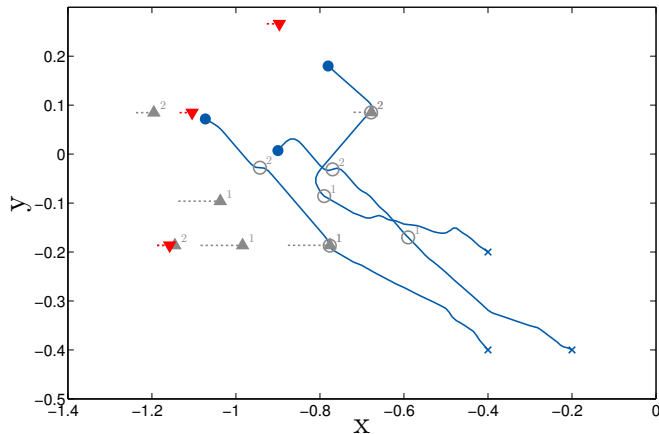
Fig. 4. Sensors (blue •) and their trajectories along with the performed measurements (gray ○) during an example simulation. Active targets (red ▼) and past targets (gray ▲) are depicted with their velocity-induced trajectories. The numbers indicate the generation that targets and measurements belonged to.

far away from their targets, the measurements at their current positions generally provide a sufficient amount of new information and improved target locations can be computed. Nevertheless, this situation might be improved by limiting the domain for target generation to the local environment of the vehicles. This would result in a loss of global information gain, but would enhance cooperation and shorten travel times between measurement locations.

6. CONCLUSION

A new adaptive observation strategy for online estimating the state of a dispersion process was proposed. It employs a PDE-based process model, adaptive generation of observation points using the ETKF as well as optimal cooperation among multiple mobile sensors provided by an MLD-based model-predictive controller. Compared to other observation schemes, the proposed approach not only produces a significantly larger error reduction, it is also more efficient with respect to the number of required measurements.

In order to avoid a central point of failure, reduce the computational effort, and improve the flexibility of the mobile sensor network, it is desirable for future work to apply a distributed observation strategy, where each sensor processes only local information. The approach presented in this paper can be seen as a starting point towards such a distributed application: While the authors already presented a possible distributed variant of the cooperative controller (Kuhn et al., 2011), the decentralization of simulation, estimation and observation point generation is subject of active research.

REFERENCES

Bemporad, A. and Morari, M. (1999). Control of systems integrating logic, dynamics, and constraints. *Automatica*, 35, 407–427.

Bishop, C. (2001). Adaptive sampling with the ensemble transform Kalman filter. Part I: Theoretical aspects. *Monthly weather review*, 129(3), 420–436.

Buizza, R. and Montani, A. (1999). Targeting observations using singular vectors. *Journal of the Atmospheric Sciences*, 56(17), 2965–2985.

Daescu, D.N. and Navon, I.M. (2003). Adaptive observations in the context of 4D-Var data assimilation. *Meteorology and Atmospheric Physics*, 85(4), 205–226.

Demetriou, M. and Ucinski, D. (2011). State estimation of spatially distributed processes using mobile sensing agents. In *Proc. of the American Control Conf.*, 1770–1776.

Duckham, M., Nittel, S., and Worboys, M. (2005). Monitoring dynamic spatial fields using responsive geosensor networks. In *Proc. of the 13th Annual ACM Int. Workshop on Geographic Information Systems*, 51–60.

Dunbabin, M. and Marques, L. (2012). Robotics for environmental monitoring: Significant advancements and applications. *IEEE Robotics & Automation Magazine*, 19(1), 24–39.

Evensen, G. (1994). Sequential data assimilation with a nonlinear quasi-geostrophic model using Monte Carlo methods to forecast error statistics. *Journal of Geophysical Research: Oceans*, 99(C5), 10143–10162.

Houtekamer, P.L. and Mitchell, H.L. (2001). A sequential ensemble Kalman filter for atmospheric data assimilation. *Monthly Weather Review*, 129(1), 123–137.

Hover, F.S. (2009). Path planning for data assimilation in mobile environmental monitoring systems. In *Proc. of the IEEE/RSJ Int. Conf. on Intelligent Robots and Systems*, 213–218.

Kalman, R.E. (1960). A new approach to linear filtering and prediction problems. *Journal of Fluids Engineering*, 82(1), 35–45.

Kuhn, J., Reinl, C., and von Stryk, O. (2011). Predictive control for multi-robot observation of multiple moving targets based on discrete-continuous linear models. In *Proc. of the 18th IFAC World Congress*, 257–262.

Lorenz, E.N. and Emanuel, K.A. (1998). Optimal sites for supplementary weather observations: Simulation with a small model. *Journal of the Atmospheric Sciences*, 55, 399–414.

Simic, S.N. and Sastry, S. (2003). Distributed environmental monitoring using random sensor networks. In *Proc. of the 2nd Int. Workshop on Information Processing in Sensor Networks*, 582–592.

Song, Z., Chen, Y., Liang, J., and Ucinski, D. (2007). Optimal mobile sensor motion planning under nonholonomic constraints for parameter estimation of distributed systems. *Int. Journal of Intelligent Systems Technologies and Applications*, 3(3/4), 277–295.

Stranders, R., Farinelli, A., Rogers, A., and Jennings, N.R. (2009). Decentralised coordination of mobile sensors using the max-sum algorithm. In *Proc. of the 21st Int. Joint Conf. on Artificial Intelligence*, 299–304.

Ucinski, D. (2004). *Optimal measurement methods for distributed parameter system identification*. CRC Press.

Wang, X. and Bishop, C.H. (2003). A comparison of breeding and ensemble transform Kalman filter ensemble forecast schemes. *Journal of the Atmospheric Sciences*, 60(9), 1140–1158.

Zhang, D., Colburn, C., and Bewley, T. (2011). Estimation and adaptive observation of environmental plumes. In *Proc. of the American Control Conf.*, 4281–4286.